REVIEW ARTICLE

Electromagnetic effects in high-frequency large-area capacitive discharges: A review

Yong-Xin Liu and Yu-Ru Zhang
Key Laboratory of Materials Modification by Laser, Ion, and Electron Beams (Ministry of Education), School of Physics and Optoelectronic Technology, Dalian University of Technology, Dalian 116024, China

Annemie Bogaerts
Research Group PLASMANT, Department of Chemistry, University of Antwerp, Universiteitsplein 1, BE-2610 Wilrijk-Antwerp, Belgium

You-Nian Wang[a)]
Key Laboratory of Materials Modification by Laser, Ion, and Electron Beams (Ministry of Education), School of Physics and Optoelectronic Technology, Dalian University of Technology, Dalian 116024, China

(Received 30 October 2014; accepted 26 January 2015; published 12 February 2015)

In traditional capacitively coupled plasmas, the discharge can be described by an electrostatic model, in which the Poisson equation is employed to determine the electrostatic electric field. However, current plasma reactors are much larger and driven at a much higher frequency. If the excitation wavelength λ in the plasma becomes comparable to the electrode radius, and the plasma skin depth δ becomes comparable to the electrode spacing, the electromagnetic (EM) effects will become significant and compromise the plasma uniformity. In this regime, capacitive discharges have to be described by an EM model, i.e., the full set of Maxwell's equations should be solved to address the EM effects. This paper gives an overview of the theory, simulation and experiments that have recently been carried out to understand these effects, which cause major uniformity problems in plasma processing for microelectronics and flat panel display industries. Furthermore, some methods for improving the plasma uniformity are also described and compared. © *2015 American Vacuum Society*. [http://dx.doi.org/10.1116/1.4907926]

I. INTRODUCTION

Radiofrequency (rf) capacitively coupled plasmas (CCPs) are widely used in dry etching of thin films and plasma enhanced chemical vapor deposition (PECVD) for the semiconductor equipment manufacturing and flat panel display industries.[1] In traditional capacitive discharges, the reactor is small (with typical dimensions of 200–300 mm in electrode diameter and 1–10 cm in electrode spacing) and usually driven at a conventional frequency, i.e., 13.56 MHz. Thus, traditional capacitive discharges typically operate in the electrostatic regime.[2–5] This means that the electrical characteristics of the plasma are only governed by Poisson's equation.

Recently, however, as the wafer sizes are increased from 300 to 450 mm, and in order to process large (1 m × 1 m) glass panels for active matrix LCD flat panel computer and TV screens, large-area CCP sources are urgently required.[6] Furthermore, these CCPs typically operate at a higher frequency, i.e., in the order of up to 200 MHz. This higher frequency not only produces a high plasma density,[7–9] and therefore high etching and deposition rates, but also gives rise to a reduced ion bombarding energy,[10,11] which is required in the near future to process integrated circuits with smaller critical dimensions (gate widths) and to increase the reactor throughput. Moreover, a higher frequency also permits the addition of a second, low-frequency bias voltage, for additional flexibility. Indeed, the combination of a high-frequency and a low-frequency allows independent control of both the ion flux and the ion bombarding energy in CCP reactors.[12–14] Thus, increasing both the substrate size and the excitation frequency in large area capacitive reactors becomes a trend for current plasma processing. However, if the excitation wavelength λ becomes comparable to the electrode radius and the plasma skin depth δ becomes comparable to the electrode spacing, so-called electromagnetic (EM) wave propagation effects, such as the standing wave effect and the skin effect, can become the most important limitations for processing uniformity.[6,9] In this regime, capacitive discharges cannot be described by a conventional electrostatic model.

Lieberman *et al.*[6] were the first to address EM effects in high frequency capacitive discharges by analytically solving the full set of Maxwell's equations. Three effects that lead to nonuniformity were identified.

(1) The standing wave effect: In a very high frequency (VHF) plasma reactor (i.e., frequency above 60 MHz), the source voltage applied to the rear of the electrode must excite a wave that propagates around the edges of

a)Electronic mail: ynwang@dlut.edu.cn

the electrode to enter the plasma. At this point, the resulting electric field is wave guided in the sheath at the surface of the electrode. For sufficiently short wavelengths and large substrates (i.e., under the condition when the wavelength is comparable to the substrate dimension), a constructive interference of the counter-propagating waves from the opposite sides of the electrode increases the amplitude of the electric field in the sheath at the center of the electrode, where the power deposition is thus enhanced.[15] When the standing wave effect is significant, the radial profile of the vertical electric field in cylindrical chamber can be roughly characterized by a zero-order Bessel function, $E_z(r) = E_0 J_0(kr)$, with the first zero at $kr_1 = 2.405$, where E_0 is the electric field at the axis, $k = 2\pi/\lambda$ is the wavenumber and λ is the wavelength in plasma. If the first voltage node of the standing wave effect occurs at the electrode edge, i.e., $kR = 2.405$, we obtain a driving frequency $f = 2.405c/\mu 2\pi R = c/2.6\mu R$, where $\mu = \lambda/\lambda_0$ is the so-called wavelength reduction factor and λ_0 is the vacuum wavelength. So, the condition for an evident standing wave effect is $f \geq c/2.6\mu R$. If the wavelength reduction factor $\mu = 5$,[16] and the electrode radius $R = 15$ cm, we obtain the criterion $f \geq c/2.6\mu R \approx 154$ MHz, for which the standing wave effect is significant. However, previous simulations and experimental results[15–19] showed that the wavelength reduction factor μ is a strong function of the external parameters (chamber design, power, pressure, etc.). So, the above criterion only gives a theoretical reference.

(2) The skin effect: At high electron density, when the plasma skin depth ($\delta = c/\omega_{pe}$, where c is the speed of light in vacuum and ω_{pe} is the electron plasma frequency) is comparable to the electrode spacing, the radial current at the electrodes induces an electric field in the plasma perpendicular to the reactor axis, resulting in a maximum power deposition near the plasma edges.[9,17]

So, the condition for an evident skin effect is $\delta = c/\omega_{pe} \leq d$, where d is the electrode spacing. We then have $n_e \geq \varepsilon_0 mc^2/e^2 d^2$, where e is elementary charge, ε_0 is the vacuum permittivity, and m is the electron mass. If we assume $d = 3$ cm, we obtain $n_e \geq 5 \times 10^{16}\,\mathrm{m}^{-3}$, for which the skin effect is significant.

(3) Edge effects: In VHF and large-scale capacitive discharges, not only an electrostatic edge effect exists, due to the enhancement of the edge electric field, but also an EM edge effect sometimes comes into play, due to the abrupt change of the permittivity at the radial plasma edge.[6] Both of them produce a maximum of the plasma density in the radial direction near the radial edge.[17] In general, the electrostatic edge effect enhances the peripheral plasma at low driving frequencies, when the standing wave effect is weak, and the electrostatic edge and skin effects can coexist,[9] if the plasma density is high enough, i.e., $n_e \geq 5 \times 10^{16}\,\mathrm{m}^{-3}$. As the driving frequency increases, the electrostatic edge effect will be gradually overtaken by the standing wave effect.

These effects have recently been investigated by analytical models, numerical models, and experiments (see below), and they show a strong dependence on various parameters. For example, in a typical PECVD capacitive discharge, where the electron density is moderate (order of $10^{16}\,\mathrm{m}^{-3}$), the standing wave and edge effects are dominant. On the other hand, in etching plasmas, the plasma density is typically higher (order of $10^{17}\,\mathrm{m}^{-3}$), and thus, the skin effects typically will take over from the standing wave effect.

The purpose of this paper is to review the work that has recently been carried out to address the EM effects in high-frequency large-area capacitive discharges and to summarize the methods proposed for improving the plasma uniformity caused by these EM effects. The paper is organized as follows. In Sec. II, we briefly review several models that describe the EM effect in capacitive discharges, including analytical models and numerical simulations, and we also present some experimental investigations of the standing wave effect and the skin effect. In Sec. III, the methods proposed for improving the plasma uniformity are discussed. Finally, conclusions and outlook will be given in Secs. IV and V, respectively.

II. CHARACTERIZATION OF THE EM EFFECTS

A. Theoretical analysis

The basic approach that should be considered to model the EM effects is naturally to solve Maxwell's equations in a typical reactor configuration. Lieberman *et al.*[6] considered an axisymmetric uniform slab model (perpendicular to the electrode plates), consisting of a homogeneous plasma and two symmetric vacuum sheaths, as schematically shown in Fig. 1. The plasma slab is considered as a uniform dielectric with a relative permittivity,

$$\kappa_p = 1 - \frac{\omega_p^2}{\omega(\omega - j\nu_m)}, \tag{1}$$

where the plasma frequency $\omega_p = (e^2 n_e/\varepsilon_0 m)^{1/2}$ is independent of r and z, and ν_m is the electron-neutral momentum

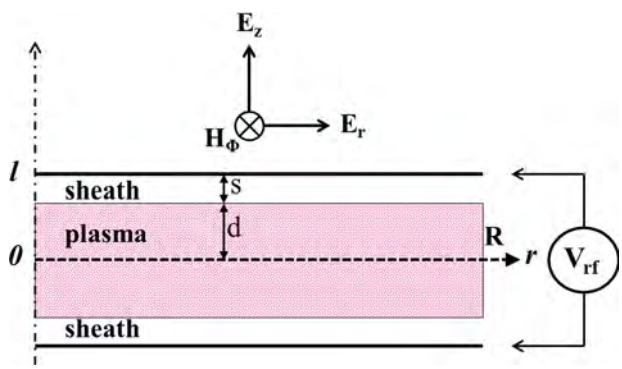

FIG. 1. (Color online) Uniform slab model of an axisymmetric discharge, considered in Ref. 6. The plasma is a uniform slab with radius R, constant half-thickness d and fixed dielectric constant, and the sheaths are vacuum regions with a fixed thickness s, with $l = d + s$. Reprinted with permission from Lieberman *et al.*, Plasma Sources Sci. Technol. **11**, 283 (2002). Copyright 2002, IOP Publishing.

transfer frequency. Considering the surface and evanescent waves propagating from the discharge edge into the center and assuming a transverse magnetic mode having only the magnetic field component $H_\phi \sim e^{j\omega t}$, the corresponding components of the electric field, E_z and E_r, are determined from Maxwell's equations

$$\frac{\partial H_\phi}{\partial z} = -j\omega\varepsilon_0\kappa_p E_r, \tag{2}$$

$$\frac{1}{r}\frac{\partial (rH_\phi)}{\partial r} = j\omega\varepsilon_0\kappa_p E_z, \tag{3}$$

$$\frac{\partial E_r}{\partial z} - \frac{\partial E_z}{\partial r} = -j\omega\mu_0 H_\phi. \tag{4}$$

Here, E_z is the capacitive electric field (perpendicular to the discharge plates) and E_r is the inductive field (parallel to the plates). Substituting E_r and E_z from Eqs. (2) and (3) into Eq. (4) yields the propagation equation for H_ϕ

$$\frac{1}{\kappa}\left[\frac{\partial^2 H_\phi}{\partial r^2} + \frac{1}{r}\frac{\partial H_\phi}{\partial r} - \frac{1}{r^2}H_\phi\right] + \frac{\partial}{\partial z}\left[\frac{1}{\kappa}\frac{\partial H_\phi}{\partial z}\right] + k_0^2 H_\phi = 0, \tag{5}$$

where $\kappa = \kappa_p = const.$ in the bulk plasma $(0 < z < z)$ and $\kappa = 1$ in the sheath $(d < z < 1)$.

After considering proper boundary conditions, the field components H_ϕ, E_z, and E_r in the bulk plasma and the sheath can be obtained by analytically solving Eq. (5). The authors found that the components of the electric field are radially and axially nonuniform due to the standing wave and skin effects, and in particular, the conditions for a uniform discharge without significant standing wave and skin effects were predicted to be $\lambda_0 \gg 2.6(l/s)^{1/2}R$ and $\delta \gg 0.45(dR)^{1/2}$, where λ_0 is the free space wavelength of the excitation frequency, $\delta = c/\omega_p$ is the collisionless skin depth, and l, s and R are defined in Fig. 1.

Sansonnens *et al.*[20] extended this study to examine the influence of asymmetric electrode areas on the EM effects, but still assumed a uniform plasma slab with vacuum sheath region. They considered a cylindrical reactor with symmetric or asymmetric electrode areas, and they also solved Maxwell's equations analytically to obtain the spatial distribution of the EM fields. They found that the so-called telegraph effect[21,22] is associated with the asymmetric electrode areas and is attributed to a redistribution of the rf current to maintain current continuity.

It is clear that the main EM effects, such as the standing wave and skin effects, can be identified by such an approach, based on an analytical solution of Maxwell's equations for a given, uniform plasma density n_e and known uniform (and arbitrarily fixed) sheath width s_m. However, the plasma density and sheath width should be determined by the particle and energy balance equations in the discharge, to be consistent with the EM field. Since the electric fields vary in the radial direction due to the standing wave effects, the plasma parameters, such as the electron density and sheath width,

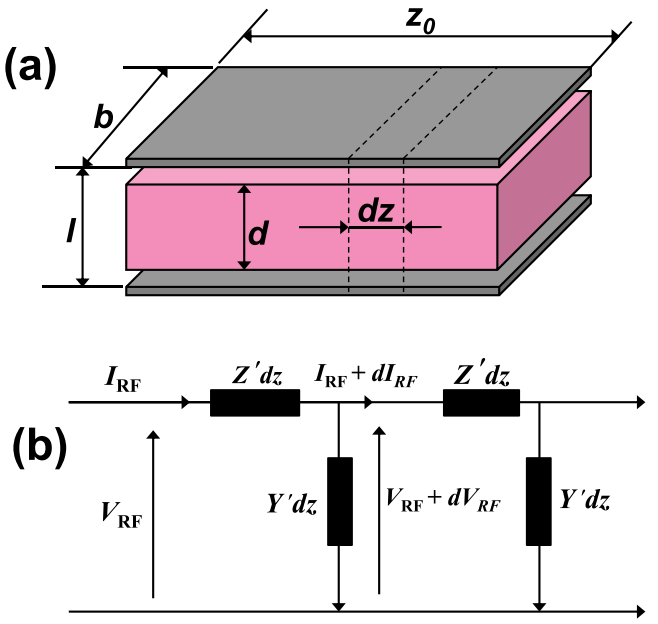

FIG. 2. (Color online) Schematic of the capacitive discharge (a) and equivalent transmission line model (b), considered in Ref. 19. Reprinted with permission from Chabert *et al.*, Phys. Plasmas **11**, 1775 (2004). Copyright 2004, American Institute of Physics.

will also vary if they are determined by the radial local particle and energy balance. A self-consistent approach was therefore developed by Chabert *et al.*[19] using a nonlinear transmission line model to analyze the EM effects. The capacitive discharge and equivalent transmission line model considered in their study are schematically shown in Fig. 2. Kirchhoff's laws applied to a slab [see Fig. 2(b)] give the transmission line equations for the current in the plates I_{rf}, and the voltage between the plates V_{rf}

$$\frac{dV_{rf}}{dz} = -Z' I_{rf}, \tag{6}$$

$$\frac{dI_{rf}}{dz} = -Y'(|V_{rf}|)V_{rf}, \tag{7}$$

where $Z' = j\omega \cdot \mu_0 l/b$ is the series impedance per unit length of the electrodes, and $Y' = 1/(2Z'_{sh} + Z'_p)$ is the parallel admittance per unit length of the sheath and the plasma. The parallel admittance per unit length is therefore the inverse of the sum of one bulk plasma impedance and two equal sheath impedances.

In this work, the particle and energy balance equations in the plasma slab were coupled to the transmission line model, to obtain the self-consistent characteristics of the standing wave effect. In particular, a self-consistent formula for the standing wave wavelength in the presence of a plasma was obtained

$$\frac{\lambda}{\lambda_0} \approx 40 V_0^{1/10} f^{-2/5} l^{-1/2}, \tag{8}$$

where λ_0 is the wavelength in vacuum (no plasma between the electrodes), V_0 is the voltage magnitude at the discharge

center (in volts), f is the frequency (in Hertz), and l is the electrode spacing (in m). Note that the shortening of the wavelength in the presence of plasma becomes worse as the frequency and/or the plate separation increases.

The self-consistent transmission line model was found to be in fairly good agreement with experimental measurements of the ion flux nonuniformity at high pressure (around 200 mTorr)[9] and at moderate rf power (order of 50 W). However, the model did not include the induced electric field (E_r) contribution and was therefore restricted to a moderate electron density regime (order of $10^{16}\,m^{-3}$), for which the skin effect is negligible (i.e., $\delta \gg d$). Recently, the same authors derived a more elaborated transmission line model from the EM fields, which, coupled to the Child law and to the particle and energy balance equations, allows to find a self-consistent solution for the power deposition and the plasma parameters in the entire range of λ and δ of practical interest.[23] It has been shown in literature that capacitive discharges may be inductively sustained. To be specific, at low voltage, capacitive heating dominates (the so-called E mode) whereas at higher voltage, the inductive heating takes over (the so-called H mode), such that the discharge experiences an E-to-H transition upon increasing voltage. However, in Ref. 23, the authors only treated the low-pressure limit, where the electron density radial profile is determined by nonlinear diffusion with constant ionization and the radial electron density profile [see Eq. (9)] is assumed based on the low pressure diffusion solution given by Godyak[24]

$$n_e(r) = n_{e0}\left[1 - \left(1 - h_R^2\right)\frac{r^2}{R^2}\right]^{1/2}. \tag{9}$$

However, in Ref. 25, Chabert *et al*. extended their study to the high-pressure limit, where the power deposition is local, such that the profiles of the plasma parameters, such as the electron density and temperature, follow the electric field profile. Their calculation results show that as the rf voltage increases, the plasma shows a spatial E to H transition, with the center of the discharge being in the E mode, while the edges are in the H mode. In other words, the electron density profile changes from a typical standing wave effect dominated case at moderate density (i.e., $1.5 \times 10^{17}\,m^{-3}$) to a skin effect dominated profile at higher density (above $10^{18}\,m^{-3}$). This phenomenon was also experimentally observed by Perret *et al*.[9] using the matrix of a planar probe to monitor the ion flux cartography.

Although the EM effects have been, to some extent, satisfactorily modeled by analytical theories, due to the great complexity of industrial reactor geometries, analytical theories are not sufficient to quantitatively predict the relative importance of the three effects mentioned in the Introduction. Moreover, the effect of complex gas mixtures, which may imply a large fraction of negative ions in the plasma, has not been seriously considered by analytical models up to now. To solve these issues, numerical simulations are needed for a better understanding of industrial plasma systems.

B. Numerical simulations

The results obtained by the analytical theories mentioned above clearly show the importance of the wave propagation phenomena in large area capacitive reactors. Therefore, self-consistent plasma simulations (either based on the fluid or particle-in-cell approach) which use the quasistatic Poisson equation approximation to determine the electric field are not sufficient for large area high frequency capacitive reactor modeling, and there is a clear need to develop fluid models with a full EM treatment. In the following, we will present the numerical simulation efforts that have been recently performed to address the EM effects in large-area high-frequency capacitive discharges.

Several years ago, Lee *et al*.[17] developed a self-consistent fluid simulation coupled with Maxwell's equations to examine the EM effects and the consequent plasma nonuniformity in capacitive discharges. They simulated single-frequency CCP discharges using a two-dimensional (2D) finite element method, which solved the coupled Maxwell's equations (in the frequency domain), the fluid plasma equations (in the time domain) and a sheath model. To simplify the bulk plasma model, the plasma was assumed to be ambipolar and quasineutral ($\Gamma_e = \Gamma_i = \Gamma$ and $n_e \approx n_i = n$), eliminating the need to solve the Poisson equation. A one-dimensional (1D) analytic collisional sheath model was employed to determine the sheath parameters and to incorporate stochastic heating effects into the electron power deposition. In this work, the authors presented some representative results for conditions where the EM effects, such as the standing wave and skin effects, are important, and the coupling of the EM effects and the electrostatic edge effects were also discussed. The self-consistently calculated radial plasma density profiles (see Fig. 3) were in good agreement with recent experimental data.[9] In particular, at 200 MHz and 150 mTorr, the authors observed a multiple voltage nodes structure of the standing wave effect, as is shown in Fig. 3. The profile shifts from a typical standing wave effect-dominated case at moderate density ($n_{e0} = 1.9 \times 10^{17}\,m^{-3}$) to a skin effect-dominated profile at higher density ($n_{e0} = 6.8 \times 10^{17}\,m^{-3}$), coupled with the edge effect. It should be noted that this fluid model showed similar results as previously obtained by the transmission line model of the standing wave and skin effects,[25] although the edge effects were neglected and purely radially local power deposition and collisionless sheaths were assumed in Ref. 25.

At the same time, Rauf *et al*.[26] developed a 2D fluid model coupled with Maxwell's equations to understand the physics of VHF CCPs. Instead of solving Maxwell's equations in a complete form, they used the electric scalar potential ϕ and magnetic vector potential $\mathbf{A}$ to represent the fields, which helps to simplify the computational solution. Their results show that the plasma spatial profile is influenced by both electrostatic and EM effects (see Fig. 4). And the relative importance of EM and electrostatic effects was found to be a function of the rf source power, the interelectrode gap and the plasma electronegativity (or gas mixture). Especially, the authors found that the peak of the electron

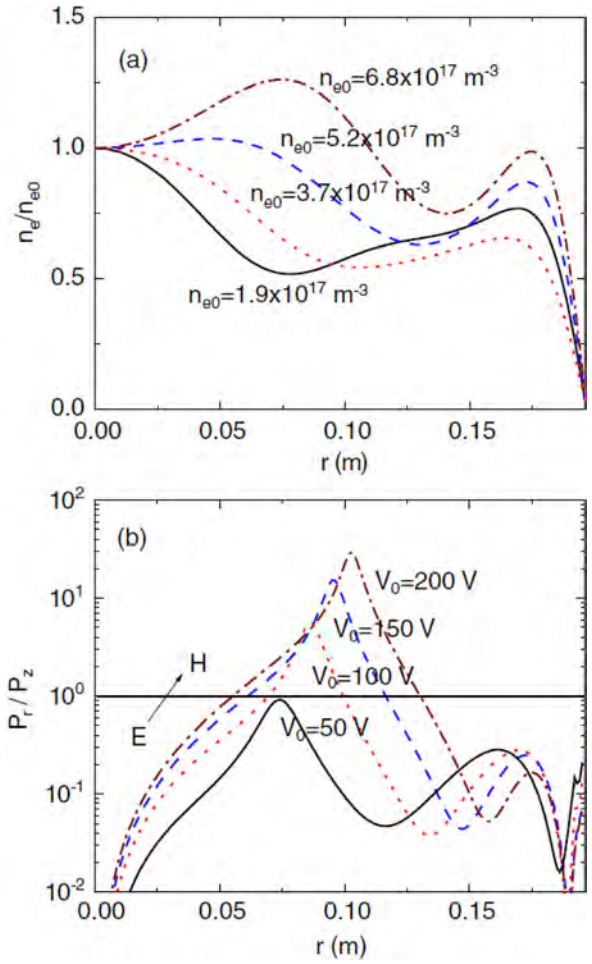

FIG. 3. (Color online) Radial profiles of (a) the electron density normalized to its central density, for different plasma densities, and (b) the inductive-to-capacitive power ratio, for various rf voltages, at 200 MHz and 150 mTorr, as calculated with the fluid model of Ref. 17. Reprinted with permission from Lee *et al.*, Plasma Sources Sci. Technol. **17**, 015018 (2008). Copyright 2008, IOP Publishing.

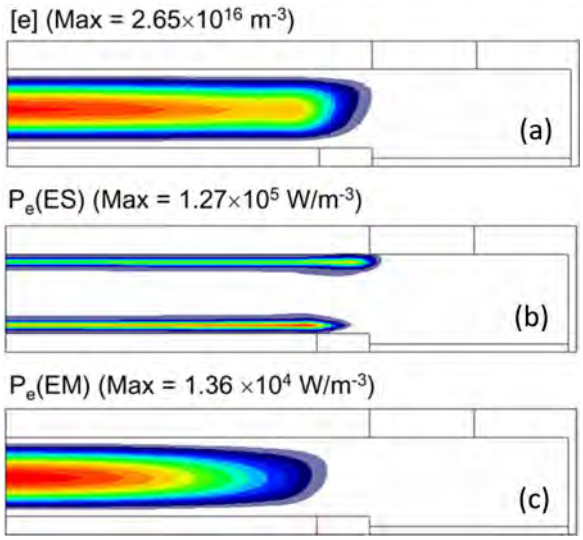

FIG. 4. (Color online) Spatial profile of electron density (a), power deposition due to the electrostatic field (b), and EM field (c), at 180 MHz driving frequency, 100 W source power, and 100 mTorr gas pressure, calculated with a fluid model of Ref. 26. Reprinted with permission from Rauf *et al.*, Plasma Sources Sci. Technol. **17**, 035003 (2008). Copyright 2008, IOP Publishing.

density shifted toward the edges of the electrodes with increasing SF_6 and CF_4 fraction from 0 to 30%, and the outward shift of the maximum in the electron density in the Ar/SF_6 plasma is more intense due to the higher electronegativity of SF_6 compared with CF_4. This observation is important, because in practical processing plasmas, gas mixtures with complex chemical properties are always employed and these plasmas are generally electronegative. The EM effects, especially the standing wave effect, in electronegative plasmas are therefore worth studying for their importance in practical use and thus more attention should be paid to these electronegative plasmas. The impact of the electronegativity on the EM effects can be explained by the change in spatial dependence of the conductivity with the addition of the electronegative gases.

A similar model was developed by Zhang *et al.*[27] to simulate the EM wave effect and its influence on the plasma uniformity in VHF capacitive discharges. They found that at 13.56 MHz, the plasma density exhibits a peak at the edge, which is caused by the electrostatic edge effect, due to the locally enhanced electrostatic field. As the frequency rises to 100 MHz, the standing wave effect becomes pronounced, and it is finally taken over by the skin effect at 200 MHz.

Yang and Kushner[15] improved the model of Rauf *et al.*,[26] and solved the full-wave Maxwell's equations, and its solution was integrated into the plasma hydrodynamics modules of the 2D Hybrid Plasma Equipment Model.[2] This enables to simulate the inductive effects that result from wave penetration at high frequency into the plasma, as well as the standing wave effects, in addition to the electrostatic effects. Under this condition, the EM fields are considered to be generated by waves launched into the reactor from the cable attached to the power supply which acts as an antenna, while the electrostatic fields are produced by spatial charges. With this model, the authors predicted the transition of the electron density radial profile from edge high to center high with increasing frequency, which is clearly due to the standing wave effect. This transition was analyzed in detail in Ref. 15. Furthermore, an extended investigation was carried out in Ref. 28, where the effects of the operating parameters (i.e., pressure, power and gas mixture) on the plasma properties in DF (dual frequency)-CCP reactors were discussed. Considering the electronegativity effects, it is worth mentioning that with the increase of the CF_4 fraction, there is an obvious decrease in the peak electron density, as is clear from Fig. 5, and in particular, an evident shift toward the electrode edge (i.e., the uniformity is becoming slightly better). This is due, in part, to the fact that the plasma-induced wavelength increases with decreasing electron density or increasing electronegativity, making the plasma more electrostatic. On the other hand, the decreasing electron density leads to an increase in the skin depth, which contributes to more bulk electron heating and so it improves the overall

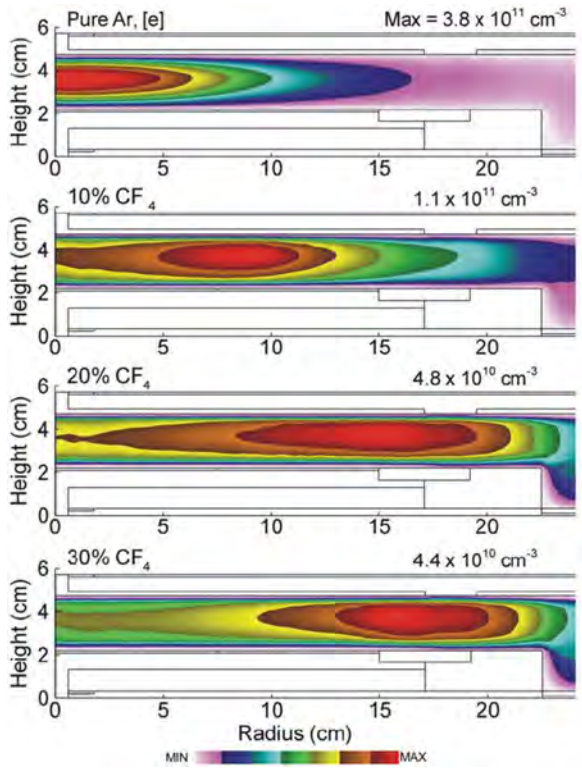

FIG. 5. (Color online) Time averaged electron density profile for CF_4 fractions of 0, 0.1, 0.2, and 0.3 in Ar (both high and low frequency powers are 300 W, high frequency is 150 MHz, low frequency is 10 MHz, 50 mTorr). Reprinted with permission from Y. Yang and M. J. Kushner, Plasma Sources Sci. Technol. **19**, 055012 (2010). Copyright 2010, IOP Publishing.

uniformity of the plasma. In addition, the ion densities (Ar^+ and CF_3^+) and their fluxes toward the wafer follow the behavior of the electrons, i.e., at a high CF_4 fraction, the radial uniformity tends to be improved.

In order to investigate the strategies for improving the chamber design, Chen *et al.*[29] applied the finite-difference time-domain method[30] to model the rf wave behavior in a cylindrical plasma etch chamber including the rf power delivery subsystem, rf feed, electrodes, and the plasma domain as an integrated system. With this method, they explored various EM wave effects and the impact of the rf feed structure on the processing uniformity. This model was later on improved to include the nonlinear plasma dynamics in a fully self-consistent way.[31] Such a 3D self-consistent EM model for CCPs could provide a complete understanding of the EM wave effects in a large-area rectangular plasma reactor having enough resemblance to real-world industrial plasma chambers. In their results, various higher-order electromagnetic modes of the EM fields can be excited in a large-area rectangular reactor upon increasing the driving frequency or rf power. The higher-order electromagnetic modes can create not only a center-high plasma distribution but also a high plasma density at the corners and along the edges of the reactor.

It should be noted that the aforementioned studies on understanding the EM wave effects in large-area high-frequency CCP reactors are mostly focused on the fundamental excitation frequency, its standing wave effect in the reactor, and the corresponding influence on the plasma uniformity. However, analyzing the standing wave effects at the fundamental excitation frequency does not explain the observation of a sharp center-peaked profile in semiconductor processing reactors with wafer radius of ~10 cm driven at 60 MHz.[32] For this purpose, a high-resolution fluid model coupled with plasma-EM wave governing equations was developed by Upadhyay *et al.*[32,33] The computational meshes (in space and time) were very small, providing adequate spatiotemporal resolution to resolve the higher harmonic EM wave contents and to investigate the effect of the higher harmonics of the EM field on the plasma density radial profiles. The calculated spatial profile of the plasma density showed a qualitative agreement with the experimental observation of a sharp center-peaked electron density profile, and especially, the frequency spectrum of the axial electric field obtained from its fast Fourier transform, is very likely a reproduction of the phenomena experimentally observed by Miller *et al.*[34] The sharp center-peaked profile is believed to be highly correlated with the higher harmonics, as is shown in Fig. 6. However, how the higher harmonics evolve from the fundamental excitation frequency is still not clear.

To conclude, it is evident that in the past few years, a considerable progress has been made to improve the fluid models used to simulate the EM effects in complex process chambers. For example, more simplified fluid models based on solving Poisson's equation[17] are replaced by complete fluid equations,[26] and simplified calculations of the EM fields based on the electric scalar potential and magnetic

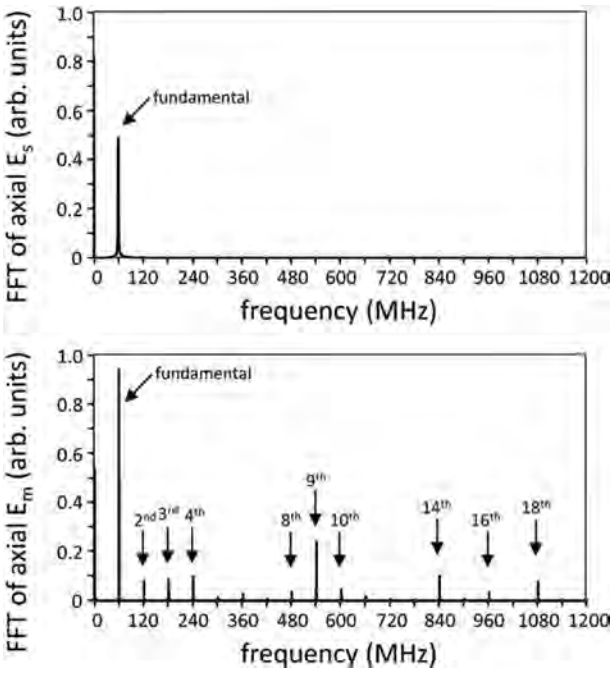

FIG. 6. FFT spectrum of the axial electric field in the midgap axial location of the reactor for a 100 mTorr argon discharge driven at 60 MHz, calculated with the fluid model of Ref. 32. Top: FFT spectrum of the electrostatic field, obtained with the plasma-electrostatics model. Bottom: FFT spectrum of the EM field in the coupled plasma-EM wave model. Reprinted with permission from Upadhyay *et al.*, J. Phys. D: Appl. Phys. **46**, 472001 (2013). Copyright 2013, IOP Publishing.

vector potential to represent the fields[26] are replaced by solving the full-wave Maxwell's equations,[15] and the EM fields are considered to be generated by waves launched into the reactor from the location of rf connection. Moreover, simple parallel plate chambers with simple rf power feeding pattern are replaced by geometries, which highly resemble real-word process chambers, as described in Ref. 15.

Up to now, the EM effects in high frequency large area capacitive discharges have been primarily described by pure fluid models coupled with full-wave Maxwell equations, or integrated into a hybrid model.[15,28] Most of these studies focus on the spatial profile of the electric field dominated by the EM effects and its influence on the plasma spatial uniformity, but the underlying physics, i.e., the electron heating mechanisms, related to the EM effects, have not been investigated in so much detail. To better address these issues, the calculation of the two- or three-dimensional EM fields should be coupled to particle in cell simulations in the future, so that plasma kinetic effects could also be included.

C. Experimental diagnostics

Experimental diagnostics are crucial to directly analyze the EM effects in real-world plasma processing reactors and to verify the reliability of the proposed analytical and numerical models. A standing wave effect was already observed in experiments by Perret *et al.*,[9] by measuring the nonuniformity of the ion flux toward the electrode in a large-area square (40 cm× 40 cm) capacitive discharge, sustained in argon at 150 mTorr and driven at frequencies between 13.56 and 81.36 MHz. As shown in Fig. 7, center-peaked ion fluxes are observed at 60 MHz and become pronounced at 81.36 MHz, due to the standing wave effect. On the other hand, at higher power (170–265 W) and higher plasma densities, the skin depth for the electric field penetration becomes proportional to the electrode spacing. At that point, electrode-edge-peaked ion fluxes are observed due to the skin effect or due to a contribution from the electrostatic edge effects, which yield the highest power at this location.

Perret *et al.*[10] later measured the ion energy distribution functions, by means of three retarding field energy analyzers, at the center, the side and the corner of the electrodes in the same discharge reactor at 81.36 MHz and 15 mTorr. Their most important observation was that the peak (around 35 V) is independent of the location of the analyzer, which means that the ion energy is uniform, even though the rf voltage and the ion flux are strongly nonuniform, as observed from the probe measurements.[9] The authors deduced that this uniform ion energy across the reactor was attributed to the dc current flowing in the radial direction in the plasma and in the electrodes. This assumption was later confirmed by Howling *et al.*[35] through measuring the dc current toward the surface of the grounded electrode. Meanwhile, Howling *et al.* pointed out that when a dielectric substrate is placed on the electrode, the dc current cannot flow in the radial direction in the electrode and therefore the ion energy will not be uniform.

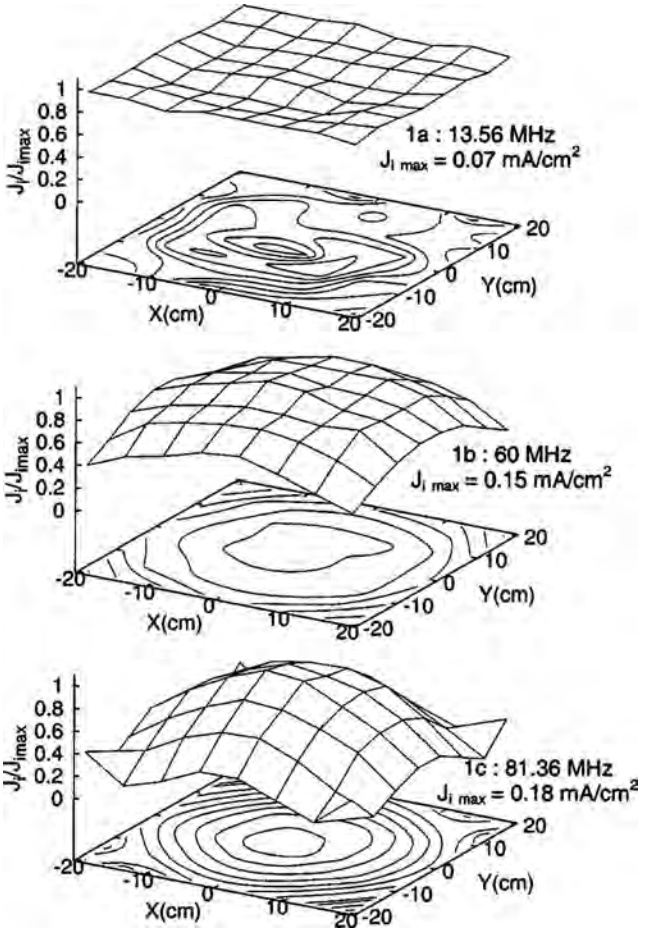

FIG. 7. Measured 2D ion flux uniformity toward the wafer, at 150 mTorr and 50 W, for different frequencies. Reprinted with permission from Perret *et al.*, Appl. Phys. Lett. **83**, 243 (2003). Copyright 2003, American Institute of Physics.

Hebner *et al.*[36] experimentally investigated the characteristics of a dual-frequency, capacitively coupled, 300 mm-wafer plasma processing system, operating in argon and driven over a wide range of frequencies between 10 and 190 MHz. In particular, they found that the radial distribution of the ion saturation current from a probe changed from uniform to center peaked, at rising excitation frequency. This was explained by a drop in the wavelength with increasing frequency, due to the standing wave effect.

A more direct evidence of the standing wave effect was presented by Barnat *et al.*[37] by measuring the radial profile of the peak voltage drop across a sheath between a 300 mm electrode and an argon plasma. The voltage drop across the sheath was derived by the integration of the electric field within the sheath, which was measured by using laser-induced fluorescence-dip spectroscopy.[38] As illustrated in Fig. 8, at a lower frequency of 13.56 MHz, the voltage drop across the sheath was uniform across the 300 mm electrode, while at higher frequencies of 60 and 162 MHz, the voltage drop becomes radially nonuniform. Especially in the 162 MHz case, the authors could not detect the electric fields near the edge of the electrode, where the potential drop across the sheath was expected to be quite small.

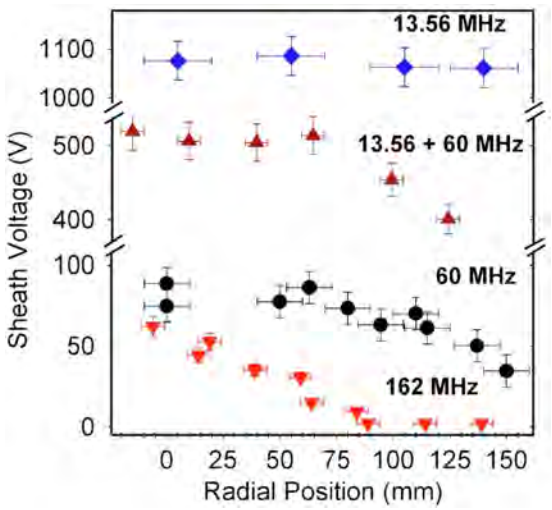

FIG. 8. (Color online) Radial dependence of the measured potential drop across a sheath formed between a 300 mm-diameter electrode and a capacitive discharge for different frequencies. Reprinted with permission from Barnat *et al.*, Appl. Phys. Lett. **90**, 201503 (2007). Copyright 2007, American Institute of Physics.

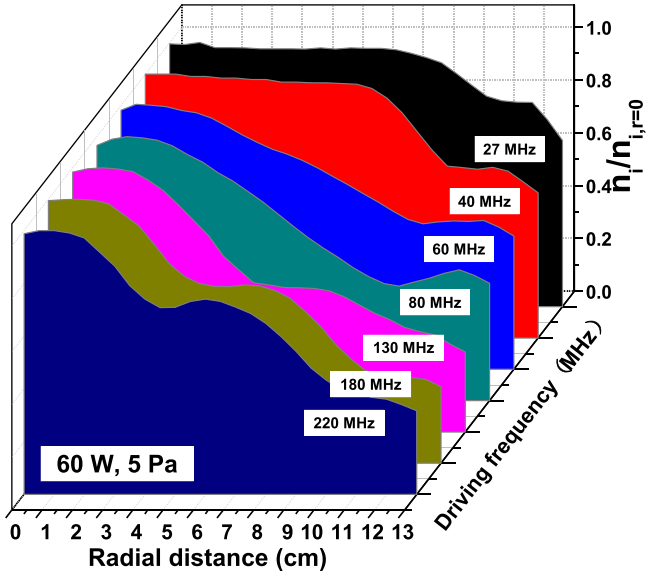

FIG. 9. (Color online) Measured radial profile of the plasma density along the reactor midgap for different driving frequencies. The density curves are all normalized to their central values. Reprinted with permission from Liu *et al.*, J. Appl. Phys. **116**, 043303 (2014). Copyright 2014, American Institute of Physics.

Higher harmonic phenomena were observed by Miller *et al.*,[34] by measuring the magnetic field in the same plasma reactor as in Ref. 36, by means of a B-dot probe. The magnetic field was measured at different spatial positions and frequencies. By means of fast Fourier transform of the B-dot signals, the authors presented up to the 10th harmonics of the EM wave for various fundamental excitation frequencies, i.e., 13.56, 60, and 176 MHz. The authors attributed the existence of the higher harmonics to the complex interactions between the external circuit driving the reactor and the nonlinear sheaths. A similar phenomenon was actually later observed in the high-resolution computational model presented in Refs. 32 and 33, showing the existence of higher harmonics of the axial electric field (see also above). These higher harmonics were believed to be highly correlated with the sharp center-peaked electron density profile.[32]

Because transmission line theory[25] and self-consistent fluid simulations[17] have previously predicted the multiple-node structure of the standing wave effect, some experiments have been performed at this high frequency (~200 MHz),[34,36] but no experiment was able to confirm these theories and simulation predictions. Indeed, the plasma parameters always seemed to monotonously decrease with radial distance. Very recently, however, Liu *et al.*[18] observed the multiple-node structure of the standing wave effect, and examined the relation between the rf power and the standing-wave wavelength (see Fig. 9). They also found that the plasma density exhibits a peak at the electrode edge, which is believed to be the EM wave attenuation effect. Hence, these measurements confirmed the previous results obtained by theory and simulation.[18,25]

In general, we can conclude that the EM effects, predicted by theory and simulation, have been confirmed by experiments, most of which are based on measuring the ion flux toward the electrode, the emission intensity (spatially integrated along the interelectrode spacing) and the radial profile of the plasma density (by using an electrostatic probe). Although these quantities are derived from the spatial profiles of the EM fields, and therefore give some insight in the EM effects, a more desirable method to better understand the EM effects would be to directly measure the electric and magnetic fields, which determine the local power deposition profile and consequently the plasma density spatial profiles. To the best of our knowledge, such experiments have not been reported yet. A B-dot probe was employed by Ahn and Chang[39] to measure the inductive electric field (i.e., time-varying magnetic field), but this experiment was performed in a small plasma chamber (14 cm in electrode diameter) and the driving frequency was not high enough (<90 MHz) for the standing wave and skin effects to become significant. Nevertheless, we believe that measurements based on these new diagnostic tools (e. g., a B-dot probe), as well as a combination of several diagnostics, will help to improve our understanding of the EM effects in large area and high frequency capacitive discharges.

III. METHODS FOR SUPPRESSING THE EM EFFECTS

Because of the current trend of increasing both the substrate size and the driving frequency, the plasma nonuniformity caused by the EM effects, especially the standing wave effect, has become a severe problem in practice, which would restrict the use of large-area, high-frequency plasma reactors for material processing. In order to improve the plasma uniformity, some methods have been proposed during the last decade to suppress these EM effects. These methods can be grouped into two categories, i.e., control by shaped electrodes or by the rf source parameters. A detailed

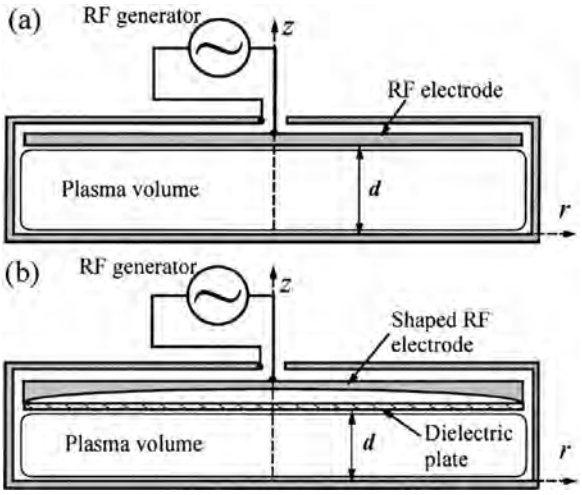

FIG. 10. (a) Cylindrical rf parallel plate plasma reactor, and (b) plasma reactor with shaped rf electrode and dielectric sheet, proposed in Ref. 40 for uniform plasma generation at high frequency. Reprinted with permission from L. Sansonnens and J. Schmitt, Appl. Phys. Lett. **82**, 182 (2003). Copyright 2003, American Institute of Physics.

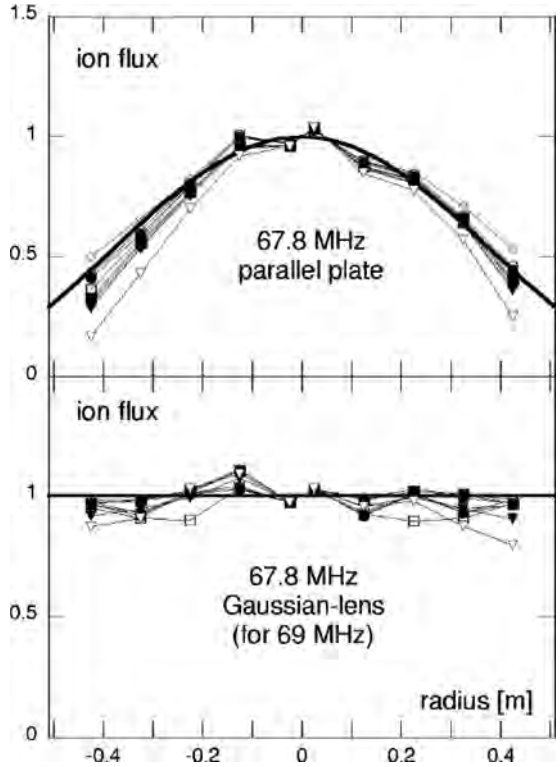

FIG. 11. Evidence of the suppression of the standing wave effect by the lens concept. Reprinted with permission from Schmidt *et al.*, J. Appl. Phys. **95**, 4559 (2004). Copyright 2004, American Institute of Physics.

description of both methods will be presented in Secs. III A and III B.

A. Control by shaped electrodes

1. Gaussian shaped electrode

A shaped electrode with a dielectric lens has been proposed by Sansonnens and Schmitt[40] to suppress the standing wave effect [see Fig. 10(b)]. The required shape of the electrode (a Gaussian shape) was determined from a solution of Maxwell's equations in vacuum; however, the authors postulated that the presence of plasma would not significantly modify the required shape, as long as the plasma density and the plasma resistivity were not too high, i.e., when the skin depth remained large compared to the plasma thickness. The Gaussian shape of the electrode, as shown in Fig. 10(b), can be described by the following equation for $k_0 d \ll 1$:

$$d = a_0 \exp(-k_0^2 r^2/4), \tag{10}$$

where k_0 is the wave number in vacuum, d is the interelectrode gap, and a_0 corresponds to the electrode gap on-axis.

The postulation that the shape calculated for the vacuum case remains valid in the presence of a plasma has recently been proven theoretically by Chabert *et al.*[41] using an equivalent circuit model. In their work, after considering the presence of plasma, the calculated shape of the electrode was identical to Eq. (10) obtained by Sansonnens and Schmitt[40] using Maxwell's equations.

Measurements of the nonuniform ion flux on the electrode, performed by Schmidt *et al.*[16] in a 1 m-diameter cylindrical reactor at 67.8 MHz have proven that this lens solution is effective for suppressing the radial standing wave nonuniformity for a wide range of plasma parameters. Figure 11 illustrates the standing wave effect on the ion flux when using parallel electrodes (see top curves), whereas a uniform ion flux is obtained when using the Gaussian electrode with lens (see bottom curves).

The Gaussian-shaped electrode proposed by Sansonnens and Schmitt[40] later proved to be only valid for reactors with cylindrical symmetry, i.e., reactors with a central rf feed connection. However, most of the large area PECVD or etching applications are performed on rectangular substrates and therefore they require large area rectangular reactors, for which the shaped electrode technique still has to be improved. Sansonnens[42] has developed a numerical method, based on a 2D quasiplanar circuit model, to calculate the electrode shape that can suppress the EM standing wave nonuniformity in the case of rectangular reactors. In particular, it was shown that the electrode shape in rectangular reactors depends not only on the reactor dimensions and excitation frequency, but also on the number and position of the rf connections on the electrodes. Experiments indeed demonstrated that the shaped electrode profile calculated with this numerical method is effective in removing the nonuniformity due to the standing wave effect in large area rectangular capacitive rf plasma reactors.[43]

The lens-shaped electrode appears to be promising for suppressing nonuniformities in the context of moderate electron densities (order of $10^{16}\,\mathrm{m}^{-3}$), e.g., in PECVD applications. However, this correction will not be effective enough at higher plasma densities (e.g., in etching plasmas), for which skin effects become significant. In addition, there are two major shortcomings that should be mentioned when the plasma is present: (1) the voltage drop within the dielectric

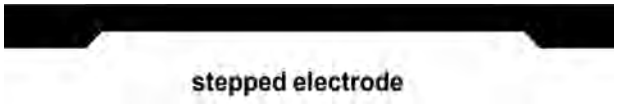

FIG. 12. Cross-section view of a stepped rf electrode.

lens is much larger than in the vacuum case, which could cause some problems if vacuum is used as the dielectric lens (e.g., a parasitic plasma may be struck in this region). (2) The calculated electrode profile has to be accurately machined; otherwise, a deviation from the ideal Gaussian profile would have a major influence on the plasma uniformity. Also, the calculated shape of the electrode is strongly frequency dependent, and thus, it will become invalid when a low frequency source is introduced.

2. Stepped electrode

In order to avoid the complex mechanical processing, which is needed for a lens-shaped electrode, a stepped electrode was proposed to suppress the standing wave effect (see Fig. 12).[44] Although the shape of the stepped electrode is not determined by a rigorous calculation, this type of shaped top electrode proved to considerably improve the etch rate uniformity, albeit in a narrow process parameter range. In practical plasma processing, the depth and diameter of the groove in stepped electrodes could be adjusted to achieve maximum uniformity.

3. Multielectrode

The plasma nonuniformity is actually caused by a large gradient of power deposition along the radius due to EM effects. Based on this, a multielectrode concept,[45] i.e., a system with two concentric electrodes, powered separately by two rf sources, as shown in Fig. 13, was proposed to control the power deposition at different electrode segments by separately adjusting the powers fed on the center and the side

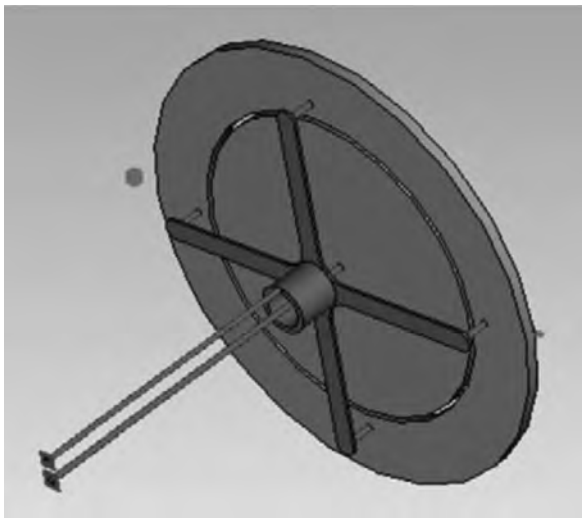

FIG. 13. Power feeding structure of the multielectrode. The electrode is split into two equal-area segments separated by a dielectric ring. Reprinted with permission from Park *et al.*, Plasma Sources Sci. Technol. **22**, 055005 (2013). Copyright 2013, IOP Publishing.

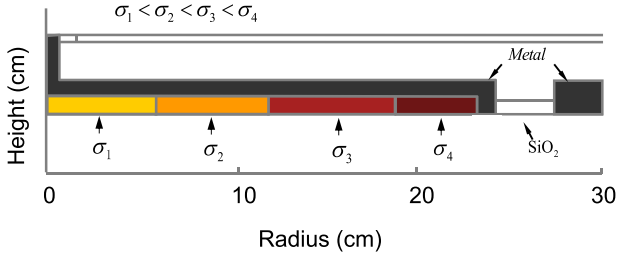

FIG. 14. (Color online) Geometry of the GCE, as studied by Yang and Kushner (Ref. 46). The metal electrode is covered by a Si plate, and the conductivity of the Si segments decreases from edge to center.

electrode. Hence, the nonuniform radial power deposition caused by the EM effects can be compensated and an optimal uniformity is obtained. The test results showed that when the powers applied to the center and side electrodes are close to each other, one can obtain the best uniformity within almost 3.5%. In practice, the ratio of the areas of the center segment to the side segment could be flexibly adjusted to achieve maximum uniformity.

4. Graded conductivity and segmented electrodes

To overcome the nonuniformity caused by the standing wave effect in real-world plasma etch chambers, Yang and Kushner[46] demonstrated by means of model computations that using graded conductivity electrodes (GCEs) can improve the plasma uniformity in a DF-CCP reactor. GCEs consist of a metal electrode covered by a dielectric, which is in direct contact with the plasma, as is shown in Fig. 14. The conductivity of the dielectric decreases from edge to center. Hence, as the HF wave propagates inwards from the edge of the electrode, the penetration of the high-frequency field into the dielectric increases due to the decreasing conductivity. This leaves a smaller fraction of the potential to be dropped across the sheath. The latter counteracts the enhancement of the HF electric field at the center of the reactor due to the standing wave effect, and thereby increases the uniformity of the HF field.

Another method that might be used to suppress the EM wave effects in 450 mm reactors is segmenting the HF electrode in order to equilibrate the distance from the rf feeds to the plasma sheath, see Fig. 15.[47] In doing so, the uniformity of plasma excitation with finite wavelengths can be improved. The reason for improving the uniformity is twofold: (1) By separately powering the segments in the same

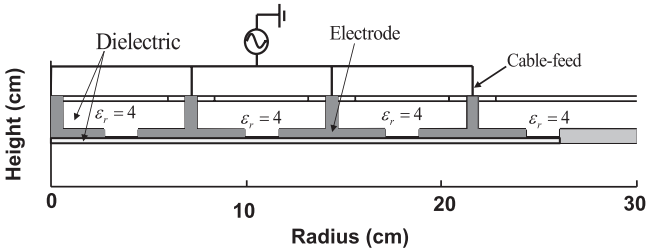

FIG. 15. Geometry of a segmented electrode, as proposed by Yang and Kushner (Ref. 15).

phase, the HF wave still propagates from the outmost edge of the electrode segment toward the center of the reactor. However, the uniformity of the HF field is improved as the distance from the rf feeds to the plasma sheath is nearly equal. (2) The ratio of the unpowered area (due to the spacing between segments) to the powered area is the largest at small radii, which decreases the fraction of the total power dissipated near the center of the reactor.

However, the phase of the segments could also be tuned to control the uniformity. Chen and coworkers[48] used a self-consistent 3D electromagnetic plasma model[31] to study the effect of segmenting the large-area electrode in improving the plasma uniformity for VHF sources. In their model, the powered large-area electrode of 2.4×2.8 m^2 is divided into an array of 3×3 subelectrodes of 0.55×0.70 m^2. Each subelectrode is fed separately at 60 MHz, and the neighboring subelectrodes are fed 180° out of phase. The modeling results show that in comparison with the strong standing wave pattern shown in their previous work,[31] the electron density across the reactor is much more uniform and the standing wave effect is essentially eliminated.

B. Control by the power source parameters

Although the electrodes with special shape can improve the plasma uniformity, in practice, these special-shaped electrodes induce a serious complication for machining the reactor. Therefore, alternative methods should be considered for improving the plasma uniformity in VHF-CCP reactors, which do not require major changes in the reactor construction, but rather allow to control the uniformity by varying some adjustable external parameters. In the following, we will present some methods which fall under this category.

1. Phase shift control

In parallel plate capacitive discharges, the top and bottom electrodes can be separately powered by two identical-frequency power supplies or by one power supply with adjustable phase difference between the voltages applied on the two electrodes, so that the uniformity can be flexibly controlled by adjusting the phase shift between the two source voltages. Bera *et al.*[49] used a 2D fluid model including the full set of Maxwell equations to examine the plasma uniformity by phase shift modulation. They found that at a phase angle $\varphi = 0$, the plasma reaches a maximum at the edge. At $\varphi = \pi$, i.e., out of phase condition, a more uniform plasma density distribution can be achieved. Xu *et al.*[50] compared the phase shift effect on the uniformity between an electrostatic and an EM case by using a similar 2D fluid model, including the full set of Maxwell equations; see Fig. 16 for an illustration of the electrode configuration. In the electrostatic case (13.56 MHz), the variation of the uniformity with phase angle showed a similar trend as in the results of Ref. 49. However, in the EM case (100 MHz), the situation is more complicated due to the standing wave effect, and the radial profiles showed the best uniformity at some phase-shift value between 0 and π, depending on other external parameters.[51–53]

The underlying physics for phase shift control, regardless of the electrostatic or EM cases, can be understood as follows: the phase shift between the top and bottom electrodes mainly affects the spatial distributions of the plasma currents, which correspond to the spatial distributions of the electron density. A schematic of the current flow in the in-phase and out-phase cases is shown in Fig. 17. In the in-phase case [$\varphi = 0$, see Fig. 17(a)], the voltage drop between the electrodes is very small. The currents flowing from the electrode to the wall are larger than to the opposite electrode, so the plasma mainly concentrates at the edge region. In the reverse-phase case [$\varphi = \pi$, see Fig. 17(b)], the voltage drop between the top and bottom electrodes is maximal and is higher than the voltage difference between any electrode and the grounded sidewall. This high voltage difference considerably enhances the current in the interelectrode space, where the plasma density is increased. Therefore, in the in-phase case, the electron density is lowest in the interelectrode space, whereas in the reverse phase case, it is highest in the interelectrode space.

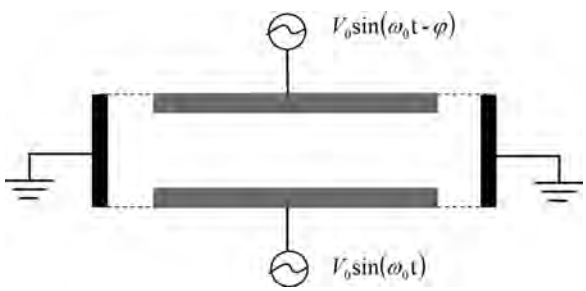

FIG. 16. Schematic diagram of a triode CCP reactor used for phase shift control.

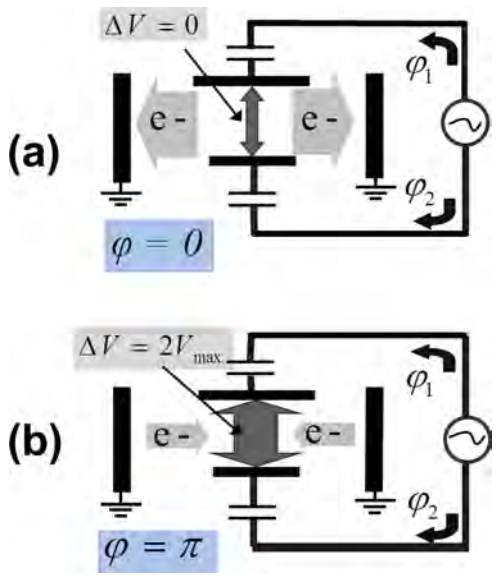

FIG. 17. (Color online) Electron flow according to the phase shift between the voltages applied to the top and bottom electrodes: (a) the current mainly flows between the electrodes and the side walls; (b) the current mainly flows between the electrodes.

In real plasma etch or deposition reactors, the phase shift control of the plasma uniformity is affected by many factors and is not exactly the same as predicted by simulations, due to the more complicated chamber geometries. The radial profiles of the plasma-emission intensity were measured by using an optical probe in a VHF-CCP triode reactor in a typical process gas mixture (i.e., $Ar/O_2/CHF_3/C_4F_6/C_4F_8$) as a function of the phase shift between the two voltages applied to the top and bottom electrodes at 100 MHz frequency (see Fig. 18).[54] It was shown that the plasma is less uniform at a phase shift $\varphi = 0$ (in-phase) and most uniform at about $\varphi = \pi$ (reverse phase). The uniformity was gradually improved upon increasing the phase shift between 0 and π. These observations are quite consistent with the simulation results in Refs. 49–53. Note that the experiments in Ref. 54 were carried out under a narrow range of process conditions (single gas pressure, fixed top and bottom VHF powers). However, the question arises whether the phase-shift control is effective under other process conditions as well, e.g., at different pressures and powers, especially under conditions adopted in practice for industrial applications. Therefore, an extended study was carried out in an industrial-type VHF-CCP reactor with a typical processing gas mixture ($C_4F_8/O_2/Ar$) in a wide range of pressures and powers.[55,56] It was shown that the phase shift corresponding to the best uniformity is strongly parameter dependent, and more importantly, the phase-shift control can considerably improve the plasma uniformity under a wide range of experimental conditions, and thus, it can be useful in industrial applications.

The phase shift control method has already been adopted by Mitsubishi Heavy Industries to improve the uniformity in a plasma process chamber with a ladder-shaped electrode.[57] Two VHF powers, between which the phase difference φ can be adjusted, are applied to a ladder-shaped electrode through multiple feeding points located at symmetrical positions of the electrode; see Fig. 19. Different from the above method, where the phase difference was fixed in one experiment, here the phase modulation method is applied by continuously alternating the phase difference from 0 to π at a frequency of 10 kHz. By using this method, one could obtain a plasma emission uniformity within $\pm 15\%$ at 60 MHz for a substrate size of 1.4×1.1 m, with nitrogen gas of 10 Pa.

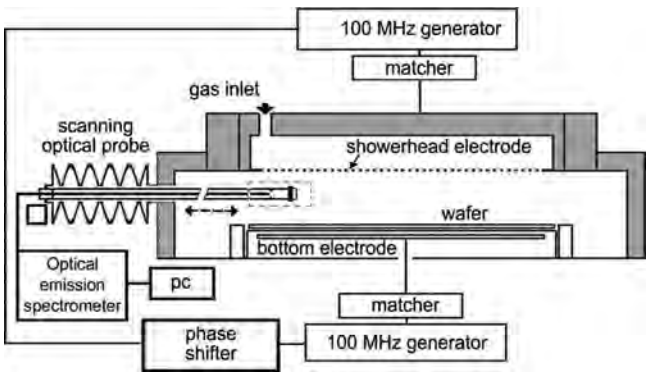

FIG. 18. Schematic of the experimental apparatus used for phase shift control. Reprinted with permission from Sung *et al.*, J. Vac. Sci. Technol., A **27**, 13 (2009). Copyright 2009, American Institute of Physics.

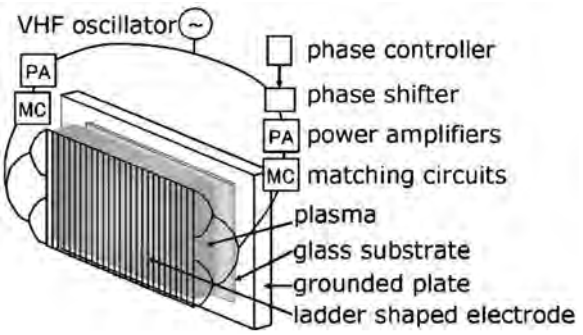

FIG. 19. Schematic diagram of the ladder-shaped electrode supplemented with phase shift control system. Reprinted with permission from Yamakoshi *et al.*, Appl. Phys. Lett. **88**, 081502 (2006). Copyright 2006, American Institute of Physics.

2. External circuit control

The external rf circuit has a significant influence on the plasma characteristics. Controlling the uniformity of VHF CCPs using external circuits is therefore a promising approach. In the early days, controlling the plasma uniformity using an external circuit was demonstrated experimentally at 13.56 MHz in the capacitively coupled Gaseous Electronics Conference reference cell by Sobolewski and Steffens.[58,59] Recently, Bera *et al.*[60] developed a 2D fluid model with external circuit to study the effects of the external circuit in controlling the VHF (60 MHz) CCP spatial profile. Plasma simulations were performed for several combinations of capacitors and inductors, and their connections to the different electrodes of the CCP reactor. It was found that the external circuit can be used to change the rf current return path, thereby modifying the plasma profile. In general, the plasma is pulled toward the electrode with an inductive impedance inserted between the top electrode and grounded electrode, and it is pushed away from the electrode with a capacitive impedance. These changes in plasma profile are related to the relative voltage and their phase on the different electrodes. Note that in the model of Bera *et al.*, the Poisson equation was solved to capture the electrodynamics; hence, EM effects were not taken into account. Nevertheless, we believe that this method could be effective to control the plasma uniformity, also when EM effects are important.

Rauf *et al.*[61] developed an EM plasma model, which includes the full set of the Maxwell equations for an asymmetric VHF CCP to understand the effect of the external rf distributed circuit on the plasma spatial profile. In their calculation configuration, the top electrode was driven by a 150 MHz VHF source, a shorted transmission line was connected to the bottom electrode, and the chamber walls were separated from the electrodes through dielectric rings (see Fig. 20). Under typical conditions, the electron density shows its peak in the center of the plasma chamber due to the standing wave effect, and the rf current from the top electrode primarily returns through the bottom electrode. When the physical length of the line or the permittivity of the dielectric filling of the transmission line was adjusted, such

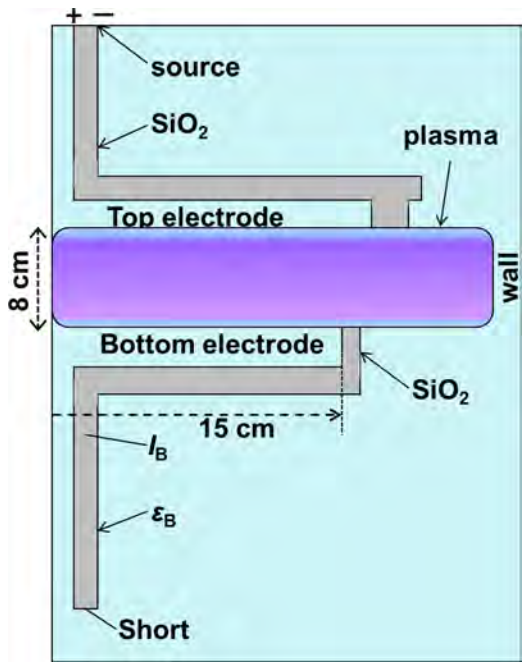

FIG. 20. (Color online) Electron density profile in the plasma reactor with the external transmission lines, as calculated by the model of Rauf *et al.* (Ref. 61).

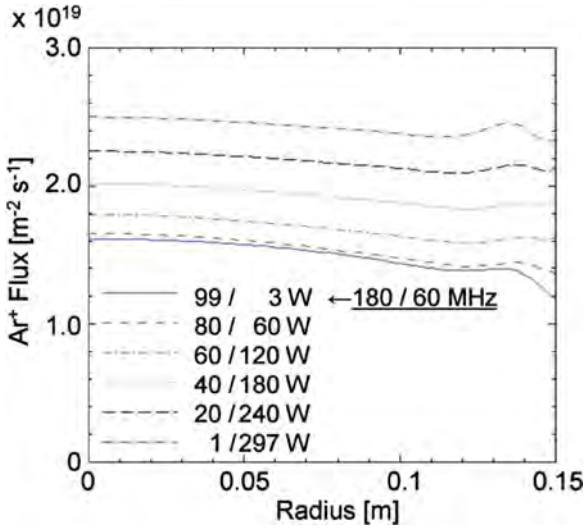

FIG. 21. (Color online) Calculated Ar^+ flux to the bottom electrode for different combinations of powers at 60 and 180 MHz. Reprinted with permission from Bera *et al.*, J. Appl. Phys. **106**, 033301 (2009). Copyright 2009, American Institute of Physics.

that it presents a large impedance (open-circuit condition) at the plasma chamber interface, the rf return current shifts from the bottom electrode to the chamber wall. As a result, the electron density peak also moves from the center toward the electrode edge. Therefore, the best uniformity could be obtained by determining the proper electrical length of the bottom transmission line.

3. Multiple VHF sources control

In the phase shift control method mentioned above, the frequency of the two VHF sources connected to the two electrodes is identical. In addition, Bera *et al.*[62] indicated that multiple VHF sources at different frequencies can also control the plasma spatial profile, specifically when the plasma distributions at the individual frequencies are different. However, the underlying physics for the two cases is quite different. In the case of two identical frequencies, the uniformity is controlled by the change of the current path between the electrode–electrode and the electrode–wall at different phase angles, which is an electrostatic effect. On the other hand, in the case of two different frequencies, it is a combination of electrostatic and EM effects. This can be understood from the simulation results of Ref. 62. In these simulations, the full set of Maxwell equations is coupled with a 2D plasma model to determine the spatial profile of the electric field and thus of the power deposition. Two VHF sources (60 and 180 MHz) were simultaneously used to excite the plasma. The simulations showed that the electron density peaks at the center of the chamber at a single frequency of 180 MHz due to the standing wave effect, while it peaks at the edges at a single frequency of 60 MHz due to the electrostatic effects. When the two rf sources are used simultaneously, and the power at 60 MHz is gradually increased, the ion flux first becomes uniform and then it changes to a peak at the electrode edge, as shown in Fig. 21. These results are confirmed by Langmuir probe measurements of the ion saturation current (not shown here). VHF mixing is therefore an effective method for dynamically controlling the plasma uniformity.

4. Other methods to control the plasma uniformity

In addition to the methods mentioned above, also many other methods were proposed by means of computer simulations and experiments. For example, Bera *et al.*[63] demonstrated that the interelectrode gap can be used to control the uniformity in a VHF CCP discharge. At large interelectrode gaps, the EM standing-wave effect is strong, and the plasma density peaks at the chamber center. As the interelectrode gap drops, the electron density increases near the electrode edge due to electrostatic electron heating, which makes the plasma more uniform in the interelectrode region.

Another viable technique to control the spatial structure of VHF CCPs is the use of an inhomogeneous magnetic field. The magnetic field can be used to enhance the plasma density near the electrode edge and to deplete the plasma in the chamber center in a controllable manner.[64]

Finally, based on the electrostatic mode (i.e., in a 13.56 MHz CCP), various structured (nonplanar) electrodes, e.g., with rectangular, rounded and triangular trenches, have been proposed and compared by Schmidt *et al.*[65] The ionization rate can be enhanced in the radial position where the electrode is trenched. Hence, a more uniform plasma can be obtained by determining one or multiple radial position(s) of trench(es) in the electrode.

IV. CONCLUSIONS

In the semiconductor and flat panel display industries, economic considerations lead to increasing substrate sizes to reduce the production costs and to increase the process throughput. Simultaneously, higher frequencies are applied to obtain a higher plasma density as well as a higher etch or deposition rate and lower dielectric damage. When a large substrate size is combined with a high excitation frequency, EM wave effects could be the dominant factor in determining the processing uniformity in plasma processing equipment. In this situation, when the excitation wavelength λ in the plasma becomes comparable to the electrode radius, and when the plasma skin depth δ becomes comparable to the electrode spacing, capacitive discharges cannot be described by the electrostatic model, and the full set of Maxwell's equations rather than Poisson's equation should be solved to address the EM effects.

These effects have been studied by using analytical EM models,[6,20] a more self-consistent transmission line approach,[19,23,25] numerical simulations,[15,17,26–28] and experiments.[9,10,36,37] The three main EM effects, compromising the plasma nonuniformity, are the standing wave effect, the skin effect and the edge effect. Based on these three EM effects, especially the standing wave effect, several researchers have proposed, based on theory, modeling or experiments, effective methods to suppress the EM effects and to improve the plasma uniformity. These methods include the use of electrodes with a special shape, such as lens-shaped electrodes, stepped electrodes, multiple electrodes, graded conductivity electrodes and segmented electrodes, as well as control of the external source parameters, such as the phase shift between the two applied frequencies, the external circuit, multiple VHF sources and so on. The effectiveness for some methods, such as the lens-shaped electrodes and the phase shift control, have been confirmed by experiments within a specific range of external parameters; however, some of these methods still remain to be tested in laboratory plasma reactors or in real process plasma reactors.

V. OUTLOOK

Although the theoretical models, numerical simulations and experimental diagnostics exhibit their respective advantages in the characterization of the EM effects, the results predicted by different methods are conflicting. For example, under similar external parameters, the plasma-induced wavelength predicted by the modelings in Ref. 17 is much smaller than that in Ref. 15. So, some simulation (or theory) results need to be further verified by the experiments, and a comparative study between simulations (or theory) and experiments is essential. However, at high frequencies, the actual power dissipated in the plasma may be much lower than the "nominal" power, which can make the comparison difficult. In addition, in order to better understand the underlying physics, i.e., the electron stochastic heating and some other effects related to the EM effects, an even more thorough examination of the 2D systems must be based on the coupling of the 2D fields and 2D PIC simulations.

There must be many additional effects when a low frequency is used. The low frequency can compress the bulk plasma and cause the bulk plasma to oscillate more intensively between the electrodes on a timescale that is long compared to the wave propagation timescale of the high frequency. Therefore, the resistance of the bulk plasma and the propagation of EM waves would change during the LF oscillations. Hence, the spatial profile of the power deposition determined by the EM effects is modulated by the low frequency.

In plasma processing, complex gas mixtures, which may imply a large fraction of negative ions in the plasma, are typically employed. The decay of the electrons in electronegative discharges causes a change in the spatial dependence of the conductivity, and thus, it can affect the propagation of waves in a subtle manner. The radial profile of the voltage in turn affects the local electron density and thus the electronegativity. Thus, a systematic study on the impact of the electronegativity on the EM effects is of fundamental and practical importance.

Finally, pulsed-modulated plasmas have been proven to demonstrate several advantages compared to continuous wave plasmas in etch processing. However, some issues associated with the use of pulsed modulation are still not clear, e.g., how do the modulation parameters (type of pulsing, pulsing frequencies, duty ratios, etc.) influence the EM effects and consequently the plasma uniformity, how will the space- and time-dependent plasma parameters look like in a pulsed plasma when the EM effects are significant, etc. All these issues should be addressed in the future.

In addition, some simulations or experiments predicted that the plasma density radial profile caused by the standing wave effect exhibits a strong dependence of the external parameters (i.e., driving frequency, applied voltage, and gas pressure), and this provides new challenges for the previously proposed methods of solving the uniformity problem, i.e., some existing methods for improving the uniformity should be re-examined or fine-tuned. For example, the Gaussian-shaped electrode is intuitively proposed based on the fact that the plasma density would monotonously decrease with radial distance, and thus, the method may become invalid when the standing wave effect presents a multinode structure, as shown in some experiments.[18] We may conclude that each method for suppressing the plasma nonuniformity has its own limitations, and only works well within a certain parameter range. In other words, one single method may not be enough to obtain a satisfying plasma uniformity in a complex industrial system; hence, a combination of different methods, e.g., a combination of a special shaped electrode and control of the external source parameters, is expected to be necessary in practical industrial chambers.

ACKNOWLEDGMENTS

This work was supported by the National Natural Science Foundation of China (NSFC) (Grant Nos. 11335004 and 11405018), the Fundamental Research Funds for the Central

Universities [Grant No. DUT13RC(3)88], and the China Postdoctoral Science Foundation (Grant No. 2014M551066).

[1]M. A. Lieberman and A. J. Lichtenberg, *Principles of Plasma Discharges and Materials Processing*, 2nd ed. (Wiley, New York, 2005).
[2]M. J. Kushner, J. Phys. D: Appl. Phys. **42**, 194013 (2009).
[3]V. Vahedi, C. K. Birdsall, M. A. Lieberman, G. DiPeso, and T. D. Rognlien, Phys. Fluids B **5**, 2719 (1993).
[4]V. Georgieva, A. Bogaerts, and R. Gijbels, J. Appl. Phys. **94**, 3748 (2003).
[5]M. A. Lieberman and V. A. Godyak, IEEE Trans. Plasma Sci. **26**, 955 (1998).
[6]M. A. Lieberman, J. P. Booth, P. Chabert, J. M. Rax, and M. M. Turner, Plasma Sources Sci. Technol. **11**, 283 (2002).
[7]E. Amanatides and D. Mataras, J. Appl. Phys. **89**, 1556 (2001).
[8]T. Kitajima, Y. Takeo, N. Nakano, and T. Makabe, J. Appl. Phys. **84**, 5928 (1998).
[9]A. Perret, P. Chabert, J. P. Booth, J. Jolly, J. Guillon, and Ph. Auvray, Appl. Phys. Lett. **83**, 243 (2003).
[10]A. Perret, P. Chabert, J. Jolly, and J. P. Booth, Appl. Phys. Lett. **86**, 021501 (2005).
[11]M. Surendra and D. B. Graves, Appl. Phys. Lett. **59**, 2091 (1991).
[12]M. Sobolewski, Y. Wang, and A. Goyette, J. Appl. Phys. **91**, 6303 (2002).
[13]H. C. Kim, J. K. Lee, and J. W. Shon, Phys. Plasmas **10**, 4545 (2003).
[14]S. Shannon, D. Hoffman, J. G. Yang, A. Paterson, and J. Holland, J. Appl. Phys. **97**, 103304 (2005).
[15]Y. Yang and M. J. Kushner, Plasma Sources Sci. Technol. **19**, 055011 (2010).
[16]H. Schmidt, L. Sansonnens, A. A. Howling, C. Hollenstein, M. Elyaakoubi, and J. P. M. Schmitt, J. Appl. Phys. **95**, 4559 (2004).
[17]I. Lee, D. B. Graves, and M. A. Lieberman, Plasma Sources Sci. Technol. **17**, 015018 (2008).
[18]Y. X. Liu, G. Fei, J. Liu, and Y. N. Wang, J. Appl. Phys. **116**, 043303 (2014).
[19]P. Chabert, J. L. Raimbault, J. M. Rax, and M. A. Lieberman, Phys. Plasmas **11**, 1775 (2004).
[20]L. Sansonnens, A. A. Howling, and Ch. Hollenstein, Plasma Sources Sci. Technol. **15**, 302 (2006).
[21]J. P. M. Schmitt, M. Elyaakoubi, and L. Sansonnens, Plasma Sources Sci. Technol. **11**, A206 (2002).
[22]A. A. Howling, L. Sansonnens, J. Ballutaud, Ch. Hollenstein, and J. P. M. Schmitt, J. Appl. Phys. **96**, 5429 (2004).
[23]P. Chabert, J. L. Raimbault, P. Levif, J. M. Rax, and M. A. Lieberman, Phys. Rev. Lett. **95**, 205001 (2005).
[24]V. A. Godyak, *Soviet Radiofrequency Discharge Research* (Delphic Associates, Fall Church, VA, 1986).
[25]P. Chabert, J. L. Raimbault, P. Levif, J. M. Rax, and M. A. Lieberman, Plasma Sources Sci. Technol. **15**, S130 (2006).
[26]S. Rauf, K. Bera, and K. Collins, Plasma Sources Sci. Technol. **17**, 035003 (2008).
[27]Y. R. Zhang, X. Xu, S. X. Zhao, A. Bogaerts, and Y. N. Wang, Phys. Plasmas **17**, 113512 (2010).
[28]Y. Yang and M. J. Kushner, Plasma Sources Sci. Technol. **19**, 055012 (2010).
[29]Z. Chen, S. Rauf, K. Ramaswamy, and K. Collins, PIERS Online **5**, 221 (2009).
[30]A. Taflove and S. C. Hagness, *Computational Electrodynamics: The Finite-Difference Time-Domain Method* (Artech House, MA, 2005).
[31]Z. Chen, S. Rauf, and K. Collins, J. Appl. Phys. **108**, 073301 (2010).
[32]R. R. Upadhyay, I. Sawada, P. L. G. Ventzek, and L. L. Raja, J. Phys. D: Appl. Phys. **46**, 472001 (2013).
[33]I. Sawada, P. L. G. Ventzek, B. Lane, T. Ohshita, R. R. Upadhyay, and L. L. Raja, Jpn. J. Appl. Phys., Part 1 **53**, 03DB01 (2014).
[34]P. A. Miller, Ed. V. Barnat, G. A. Hebner, A. M. Paterson, and J. P. Holland, Plasma Sources Sci. Technol. **15**, 889 (2006).
[35]A. A. Howling, L. Sansonnens, H. Schmidt, and Ch. Hollenstein, Appl. Phys. Lett. **87**, 076101 (2005).
[36]G. A. Hebner, Ed. V. Barnat, P. A. Miller, A. M. Paterson, and J. P. Holland, Plasma Sources Sci. Technol. **15**, 879 (2006).
[37]E. V. Barnat, P. A. Miller, G. A. Hebner, A. M. Paterson, T. Panagopoulos, E. Hammond, and J. Holland, Appl. Phys. Lett. **90**, 201503 (2007).
[38]E. V. Barnat and G. A. Hebner, J. Appl. Phys. **96**, 4762 (2004).
[39]S. K. Ahn and H. Y. Chang, Appl. Phys. Lett. **93**, 031506 (2008).
[40]L. Sansonnens and J. Schmitt, Appl. Phys. Lett. **82**, 182 (2003).
[41]P. Chabert, J. L. Raimbault, J. M. Rax, and A. Perret, Phys. Plasmas **11**, 4081 (2004).
[42]L. Sansonnens, J. Appl. Phys. **97**, 063304 (2005).
[43]L. Sansonnens, H. Schmidt, A. A. Howling, C. Hollenstein, C. Ellert, and A. Buechel, J. Vac. Sci. Technol., A **24**, 1425 (2006).
[44]D. Sung, V. Volynets, W. Hwang, Y. Sung, S. Lee, M. Choi, and G. Kim, J. Vac. Sci. Technol., A **30**, 061301 (2012).
[45]G. J. Park, S. H. Seo, C. W. Chung, and H. Y. Chang, Plasma Sources Sci. Technol. **22**, 055005 (2013).
[46]Y. Yang and M. J. Kushner, J. Phys. D: Appl. Phys. **43**, 152001 (2010).
[47]Y. Yang and M. J. Kushner, J. Appl. Phys. **108**, 113306 (2010).
[48]Z. Chen, J. Kenney, S. Rauf, K. Collins, T. Tanaka, N. Hammond, and J. Kudela, IEEE Trans. Plasma Sci. **39**, 2526 (2011).
[49]K. Bera, S. Rauf, and K. Collins, IEEE Trans. Plasma Sci. **36**, 1366 (2008).
[50]X. Xu, S. X. Zhao, Y. R. Zhang, and Y. N. Wang, J. Appl. Phys. **108**, 043308 (2010).
[51]Y. R. Zhang, X. Xu, A. Bogaerts, and Y. N. Wang, J. Phys. D: Appl. Phys. **45**, 015202 (2012).
[52]Y. R. Zhang, X. Xu, A. Bogaerts, and Y. N. Wang, J. Phys. D: Appl. Phys. **45**, 015203 (2012).
[53]Y. R. Zhang, A. Bogaerts, and Y. N. Wang, J. Phys. D: Appl. Phys. **45**, 485204 (2012).
[54]D. Sung, S. Jeong, Y. Park, V. Volynets, A. Ushakov, and G. H. Kim, J. Vac. Sci. Technol., A **27**, 13 (2009).
[55]D. Sung, J. Woo, K. Lim, K. Kim, V. Volynets, and G. H. Kim, J. Appl. Phys. **106**, 023303 (2009).
[56]V. Volynets, H. Shin, D. Kang, and D. Sung, J. Phys. D: Appl. Phys. **43**, 085203 (2010).
[57]H. Yamakoshi, K. Satake, Y. Takeuchi, H. Mashima, and T. Aoi, Appl. Phys. Lett. **88**, 081502 (2006).
[58]M. A. Sobolewski and K. L. Steffens, J. Vac. Sci. Technol., A **17**, 3281 (1999).
[59]K. L. Steffens and M. A. Sobolewski, IEEE Trans. Plasma Sci. **27**, 74 (1999).
[60]K. Bera, S. Rauf, A. Balakrishna, and K. Collins, IEEE Trans. Plasma Sci. **38**, 3241 (2010).
[61]S. Rauf, Z. Chen, and K. Collins, J. Appl. Phys. **107**, 093302 (2010).
[62]K. Bera, S. Rauf, K. Ramaswamy, and K. Collins, J. Appl. Phys. **106**, 033301 (2009).
[63]K. Bera, S. Rauf, K. Ramaswamy, and K. Collins, J. Vac. Sci. Technol., A **27**, 706 (2009).
[64]K. Bera, S. Rauf, J. Kenney, L. Dorf, and K. Collins, J. Appl. Phys. **107**, 053302 (2010).
[65]N. Schmidt, J. Schulze, E. Schüngel, and U. Czarnetzki, J. Phys. D: Appl. Phys. **46**, 505202 (2013).